Spatiotemporal behavior in a ϕ^4 model of lattice dynamics

Afshin Montakhab
Department of Physics, University of California, Santa Barbara, California 93106-9530

Jeremy Levy
Department of Physics and Astronomy, University of Pittsburgh, Pittsburgh, Pennsylvania 15260

(Received 27 May 1997)

A simple phenomenological model of lattice dynamics in ferroelectric materials has the ingredients of a spatially extended, nonlinear driven system. We study the dynamics of this model in the presence of spatially varying ultrafast optical pulses. We find that for sufficiently large amplitudes, the spatial gradient in the pulse creates stable domain walls separating domains of opposite orientations. The dynamics of these domain walls under repeated pulses is investigated. Bifurcation diagrams in one, two, and three dimensions are obtained, exhibiting both periodic and complex spatiotemporal behavior. The complex behavior is identified as weakly chaotic associated with *algebraic* growth of initial small perturbations. [S1063-651X(97)02411-2]

PACS number(s): 42.79.Vb, 63.20.Ry, 78.30.Hv, 78.47.+p

I. INTRODUCTION

In this paper we study the collective dynamics of a set of harmonically coupled, dissipative, double-well oscillators. Phonon dynamics in ferroelectric materials can be modeled as such a spatially extended nonlinear dynamical system. Fahy and Merlin have studied a simple phenomenological model in which the ferroelectric material is driven by a spatially uniform optical pulse at finite temperature [1]. They found that as the pulse strength is increased the system goes through a coherent switching behavior where the entire system changes its polarization without creation of a domain wall or fragmentation.

Here we report results for the zero-temperature version of this model under a spatially varying ultrafast pulse in a regime in which many stable domain walls can coexist. Under such conditions, we find that the model exhibits a variety of interesting spatiotemporal effects, which may also be relevant to future experimental studies of real ferroelectric materials.

Ferroelectrics are materials that exhibit a spontaneous electric polarization below a Curie temperature T_c [2]. Below this temperature, there is a spontaneous symmetry breaking of the phonon mode, leading to two or more degenerate states, separated by an energy barrier. In the model discussed here, we will assume that at very low temperatures, the dynamics of phonon amplitude ϕ can be described by a double-well potential with two correponding minima, corresponding to the two possible orientations of the electric polarization. Typically these soft modes are Raman or infrared active. Ultrafast optical pulses can therefore be used to impulsively excite and detect coherent phonons, provided that the pulse duration is short compared to the phonon period [3–5].

II. THE MODEL

A simple phenomenological model of lattice dynamics in ferroelectric materials treats the system as a set of harmonically coupled, damped oscillators [1]. Each oscillator resides in a nonlinear ϕ^4 potential $U(\phi)=\phi^4-a\phi^2$, which has a double-well structure. The height of the potential barrier between the wells is given by $a^2/4$ and the minima occur at $\phi=\pm\sqrt{a/2}$. The zero-temperature equation of motion is written as

$$m\ddot{\phi}_i = k\Delta\phi_i - 4\phi_i^3 + 2a\phi_i - \gamma\dot{\phi}_i + F_i(t), \tag{1}$$

where m is the mass, γ is the damping parameter associated with each oscillator, k is the strength of the nearest-neighbor (NN) coupling, $F_i(t)$ is the impulsive driving term, and $\Delta\phi_i=\Sigma_{j=NN}(\phi_j-\phi_i)$ is the lattice Laplacian. Here, ϕ_i represents the local phonon amplitude associated with each lattice site i so that $\phi_i=0$ is the undistorted amplitude. However, we are considering the material below the structural phase transition where a is positive so that $\phi_i=0$ is an unstable equilibrium point.

The driving mechanism is chosen to model the effect of a spatially varying ultrafast optical pulse that instantaneously changes the velocity of each oscillator with a magnitude depending on their spatial position within the lattice. We model the effect of the optical pulse by adding an impulsive driving term to the right-hand side of Eq. (1):

$$F_i(t) = \phi_i P_i \delta(t), \tag{2}$$

where P_i is the (spatially dependent) pulse magnitude. We imagine a d-dimensional square lattice and apply a symmetric pulse to the center of the lattice with a Gaussian spatial profile, $P_i=A\exp(-r_i^2/2\sigma^2)$, where A is the pulse amplitude, r_i is the distance between the center and the ith lattice, and σ sets the length scale for the pulse gradient. We emphasize that it is the spatial variation of the optical pulse that gives rise to many of the interesting results presented below.

A simple dimensional analysis gives the relevant time and length scales of the problem: $\tau\sim m/\gamma$ sets the time scale for relaxation to a metastable state—where $\ddot{\phi}=\dot{\phi}_i=0$, and $\xi\sim\sqrt{k/a}$ is the characteristic length of a domain wall separating regions of opposite orientation [6]—i.e., where $\phi=\pm\sqrt{a/2}$.

In recent years, much attention has been given to dynamics of extended systems [7]. These systems exhibit many interesting nonequilibrium phenomena including pattern formation, spatiotemporal chaos, and self-organized criticality. Nonequilibrium phenomena in extended systems are typically described by partial differential equations and/or arrays of oscillators in the form of coupled ordinary differential equations. A double-well oscillator serves as a paradigm in the study of low-dimensional chaos, and is also frequently used in numerous areas of physics [8]. Equation (1) is a natural high-dimensional generalization of a double-well oscillator. Therefore, it is important to investigate the spatiotemporal behavior of the above model.

In the following, we present results of our numerical study of the above model. In particular, we are interested in the dynamics of stable domain walls under repeated identical pulses. Does such a system exhibit complex or chaotic behavior, and if so, how does one characterize such behavior? We find that the system exhibits both periodic and complex spatiotemporal behavior. The complex regime is characterized by *algebraic* growth of small initial perturbations. Interestingly, such behavior associated with zero Lyapunov exponent has been previously shown to exist in extended systems that exhibit self-organized criticality (SOC).

III. NUMERICAL RESULTS

In this section we present the results of our numerical study of the above model. We have considered this model in various spatial dimensions; however, we have concentrated in $d=2$ and shall present most of our results for this case. An adaptive, fifth-order, Runge-Kutta method [9] was employed in order to simulate the equations of motion. We rewrite the equations of motion in cylindrical coordinates in order to take advantage of the symmetry of the problem. This allows us to simulate the radial direction only, which approximately reduces the number of equations by a factor of N (on an $N \times N$ square lattice). We are interested in the regime where many stable domain walls exist. Accordingly, we chose an intermediate coupling regime where $k \approx a$ for a large part of our simulations. We also note that in their study of the same system, Fahy and Merlin chose $k/a=20$ [1,10]. This is a strong coupling, which essentially puts the system in a ''single-particle'' regime for the system sizes they considered. The relaxation time between the application of consecutive pulses was implemented by requiring all the time derivatives to become smaller than a prespecified value ϵ, which was proportional to the accuracy of the integrator, thus assuring that the system has reached a true metastable state before a subsequent pulse is applied. We also note that in our numerical implementation, Eq. (1) is nondimensionalized in such a way that time is measured in units of γ and space in units of lattice spacing so that both A and ϕ are dimensionless.

We begin by investigating the response of the two-dimensional system to repeated pulses. We start the system from a spatially homogeneous state (i.e., $\phi_i=\sqrt{a/2}$, $\forall i$) and apply repeated pulses of a given magnitude (A) and width (σ). After each pulse, the system is allowed to relax to a metastable state where the position of each oscillator is measured and averaged over the lattice. This procedure is equivalent to measuring the average polarization in a sample. Figure 1 shows the result for such a simulation for a range of pulse strengths. The parameters chosen are $R=500$, $k=2$, $a=2$, $\gamma=0.5$, and $\sigma^2=R^2/2$, where R is the radial number of degrees of freedom (i.e., system size is πR^2 in $2d$). A large number of pulses are applied to the system so that it reaches a steady state, although typically the system settles into a periodic state after only a few pulses. Then we apply 256 pulses and plot the average polarization $\langle \phi(x,y) \rangle$ for each of the pulses. Note that for each value of A, the initial condition corresponds to the homogeneous state [10].

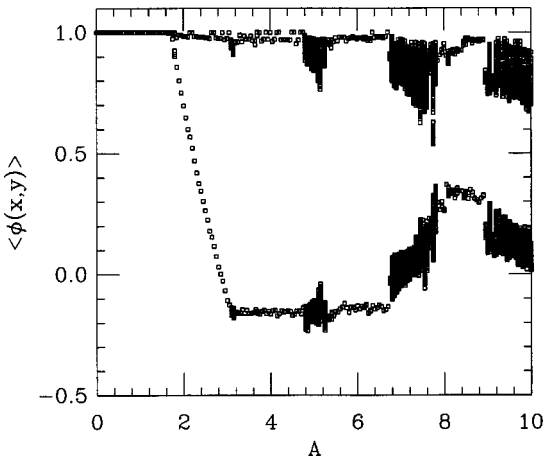

FIG. 1. Bifurcation diagram for the average final polarization as a function of pulse strength for a radially symmetric $2d$ system. Here, $R=500$, $k=2$, $a=2$, $m=1$, $\gamma=0.5$, and $\sigma^2=R^2/2$.

By plotting $\langle \phi(x,y) \rangle$ as a function of the drive amplitude A we obtain a bifurcation diagram, shown in Fig. 1. As the pulse strength is increased from zero, the system bifurcates to a period-2 state associated with the creation of the first stable domain wall at $A=1.75$. Here, when the pulse is applied to the homogeneous state, a ''bubble'' is created at the center of the pulse, with an associated domain wall separating regions of opposite orientation. The next pulse creates an additional domain wall at approximately the same location which annihilates the previous wall, leading back to a homogeneous state [11]. Thus, the period-2 behavior is associated with the creation and annihilation of a bubble at the center of the sample, while the rest of the system is unaffected.

Various snapshots of the spatiotemporal evolution of the domains for period-two behavior ($A=2.15$) are shown in Fig. 2. Initially, the system is in the uniform state, shown in Fig. 2(a). At $t=10$ units after the Gaussian pulse is applied, domain reversal occurs in the central region, as shown Fig. 2(b). The system settles into a metastable state by $t=250$ [Figs. 2(c)–2(e)], at which point a second pulse is applied. The second pulse causes a second domain reversal to occur, as seen in Fig. 2(f), which leads to the formation of a ring. Because of the close proximity of the two domains, they eventually annihilate [Figs. 2(g)–2(i)], leading back to the original state, Fig. 2(a).

As the driving amplitude A is increased, the domain wall is created at a larger distance from the center so that the size of the bubble becomes larger, as seen through the decreasing lower branch of the bifurcation diagram in Fig. 1. This trend continues until the pulse becomes strong enough to create a second set of domain walls near the center (at $A=3.1$). At

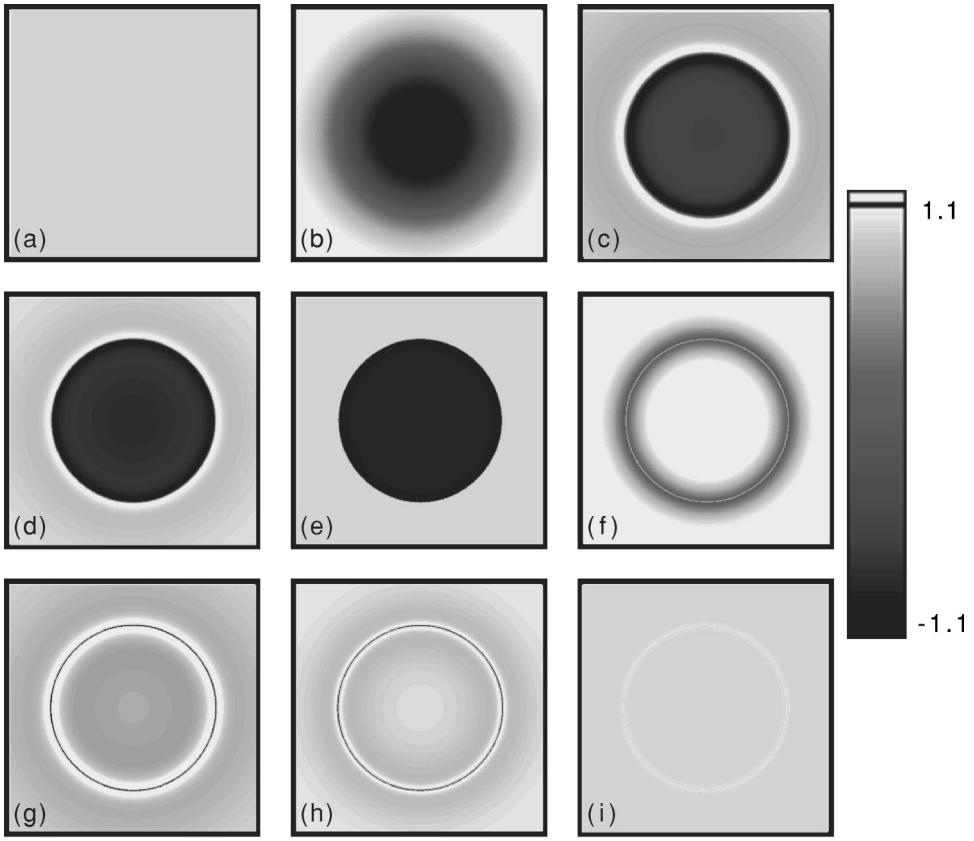

FIG. 2. Spatiotemporal evolution of the ϕ^4 model for $A=2.15$ as it goes through a period-2 motion associated with creation and annihilation of a bubble. Time t is measured from the time of the first pulse, in units of γ. (a) $t=-1$. (b) $t=10$. (c) $t=25$. (d) $t=50$. (e) $t=249$. At $t=250$, the second pulse is applied. (f) $t=260$. (g) $t=275$. (h) $t=300$. (i) $t=400$.

this point no periodic behavior is observed. As more pulses are applied to the system, the number of domain walls created near the center increases. These domain walls remain within a limited region near the center of the pulse, but nevertheless move in an irregular fashion.

As the pulse strength is increased further ($A=3.2$), the system again settles into a periodic state characterized by the creation and annihilation of a single ''ring,'' consisting of a pair of domain walls. This periodic behavior continues as the pulse strength is further increased, while the thickness of the ring remains essentially the same and its radius increases with larger pulses. At $A=4.8$, the pulse is again strong enough to create a new set of domain walls near the center. A complex spatiotemporal zone near the center of the system emerges where the pulse continues to create more and more domain walls. The width of the second complex zone is larger in size than the the first one, and in general these regions increase with increasing A.

We have looked at bifurcation diagrams in many different parameter regimes, and the above-mentioned behavior seems to be a general property of this model. The bifurcation diagrams consist of periodic regimes, associated with creation and annihilation of a small number of domain walls (e.g., one domain wall equals a bubble, two domain walls equal a ring), separated by regions that are characterized by complex interaction among many domain walls. Fig. 3 shows a representation of the general behavior of the system as a function of A.

We now focus our attention on the spatiotemporally complex behavior exhibited by this model. A space-time plot of the first complex regime is shown in Fig. 4(a), where we plot the state of the system after relaxation has occurred for the first 250 pulses. The intensity of this space-time plot designates the value of $\phi(i)$, with black corresponding to one minimum and white corresponding to the other. The elapsed time, measured in units of the number of pulses, is plotted

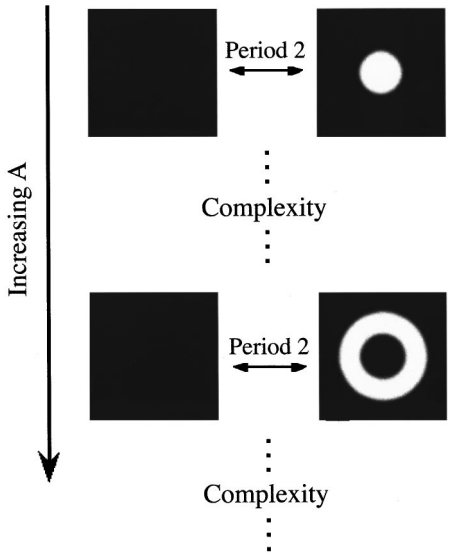

FIG. 3. A schematic representation of the state of the system as the pulse amplitude is increased.

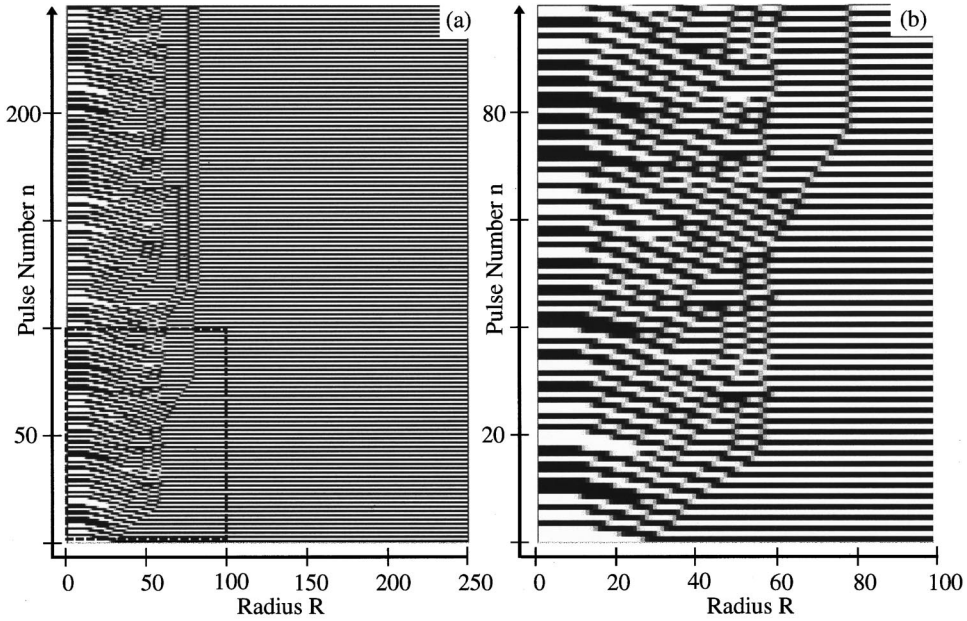

FIG. 4. Space-time plot of the complex behavior of the system at $A=3.1$ from Fig. 1. The horizontal direction (left to right) is the half radius (the first 250 radial sites) and the vertical direction (bottom to top) is time for the first 250 pulses. The plotted intensity is such that black corresponds to the positive well $(+1)$ and white to the negative well (-1). (b) Closeup of the lower-left corner, as designated by the dashed lines in (a).

vertically, increasing from bottom to top. A closeup of the lower left corner, designated by the dashed box, is shown in Fig. 4(b). For Fig. 4, $A=3.1$, while the rest of the parameters are the same as Fig. 1. The central zone (left side of the figure) contains the complex spatiotemporal behavior consisting of many interacting domain walls. Further out (to the right of the figure), the system exhibits a period-2 behavior as the domains switch orientation after each pulse. Close to the edge (not shown), the system is unaffected by the pulse. As more pulses are applied to the system, more and more domain walls are created in the complex zone near the center. These domain walls subsequently move out and are eliminated at seemingly random space-time locations. Note that the profiles plotted here are relaxed configurations that correspond to the existence of stable domain walls as opposed to the continuous time dynamics shown in Fig. 2.

As discussed above, with increasing A this first complex regime gives way to a period-2 behavior associated with creation and annihilation of a ring (see Fig. 3), which is followed by a second complex regime. Figure 5 shows a similar space-time plot of this second complex regime for the first 250 pulses and $i=0-250$ at $A=4.9$. As can be seen from the left edge of the figure, in the steady state, a new domain wall is created near the center after every fourth pulse. As these domain walls move out towards the edge, their interactions lead to a complicated pattern seen in the middle section of Fig. 5. The behavior here seems less complex than that of Fig. 4 associated with the first complex regime. Correspondingly, the behavior just outside the complex zone (right side of the figure) is simpler here than that of Fig. 4. The rest of the system (not shown) simply executes a period-2 motion associated with creation and annihilation of a ring.

This type of irregular behavior occurs for a range of A until the system again finds a periodic regime. As discussed above (and is evident from Fig. 1), the bifurcation diagram consists of regimes of periodic behavior associated with creation and annihilation of a few domain walls, followed by regimes where many interacting domain walls exhibit complex spatiotemporal behavior. The complex regime begins at the point where the pulse is just strong enough to create a new stable domain wall which can interact with a preexisting domain wall. For this reason, complex behavior is not observed at the first bifurcation point $(A=1.75)$ where only a single domain wall is created. For the sake of completeness, we show two more space-time plots. Figure 6(a) shows the rich spatiotemporal behavior associated with $A=6.8$ of Fig. 1. This is to be compared with Fig. 4. Again, a closeup of the behavior near $r=0$ and $t=0$ is shown in Fig. 6(b). Domain walls are created near the center and move through a larger complex zone. Moving away from the center, they slow down and eventually stop moving as the pulse

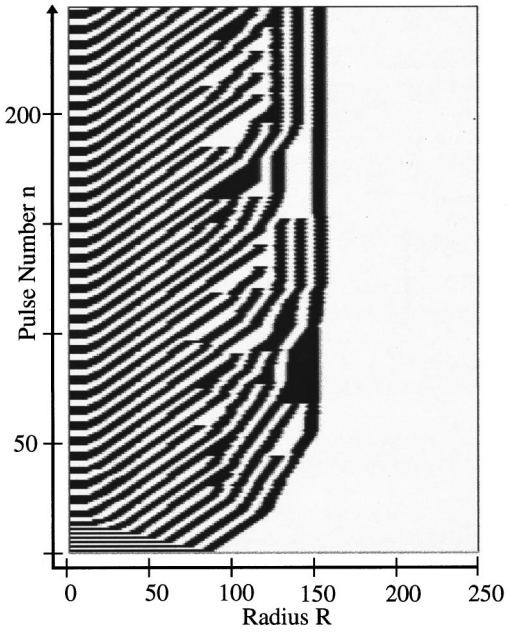

FIG. 5. (a) Space-time plot of the complex behavior of the system at $A=4.9$ from Fig. 1. The horizontal direction (left to right) is the half radius (the first 250 radial sites) and the vertical direction (bottom to top) is time for the first 250 pulses. The plotted intensity is such that black corresponds to the positive well $(+1)$ and white to the negative well (-1).

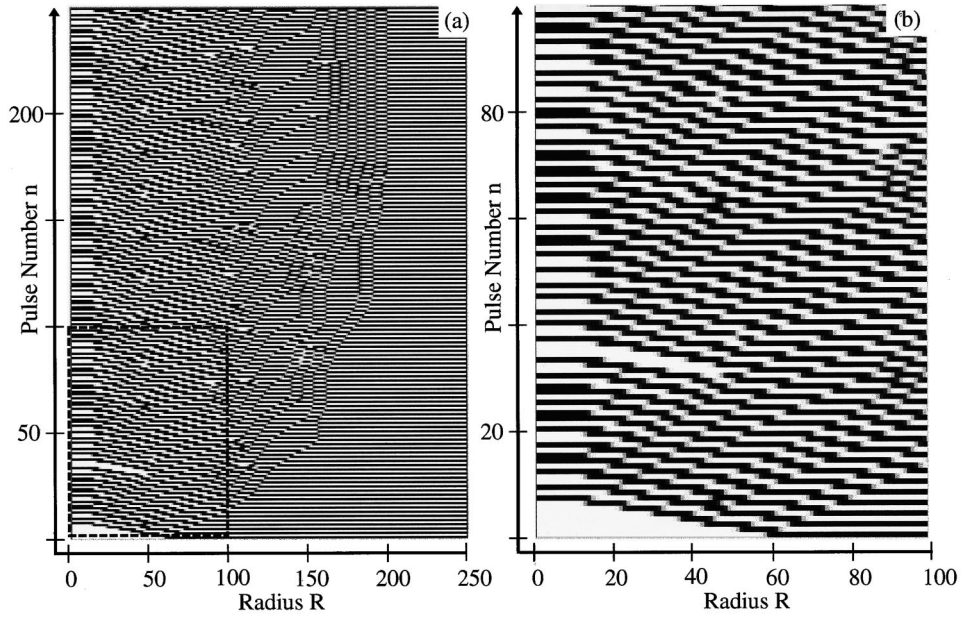

FIG. 6. (a) Space-time plot of the complex behavior of the system at $A=6.8$ from Fig. 1. The horizontal direction (left to right) is the half radius (the first 250 radial sites) and the vertical direction (bottom to top) is time for the first 250 pulses. The plotted intensity is such that black corresponds to the positive well $(+1)$ and white to the negative well (-1). (b) Closeup of the lower-left corner, as designated by the dashed lines in (a).

gradient becomes small. Throughout this complex zone, domain walls pair annihilate at seemingly random space-time locations.

Bifurcation diagrams for other system parameters were also obtained, which displayed the same type of behavior as that of Fig. 1, i.e., complex regimes separated by regimes of periodicity. In Fig. 7, we show another space-time plot from such a system. Here, domain walls are generated away from the center and move in both directions. However, the primary dissipation mechanism occurs as the walls move quickly towards the center (left side of the figure) and disappear. We emphasize that these complex regimes do not seem to be transients, as we have applied thousands of pulses for select parameters and observed no convergence to any type of regular behavior [12].

In the above space-time plots the repulsive interaction between nearby domain walls is to be noted. For example, in Fig. 6, the outermost wall (i.e., the wall created after the first pulse) initially moves out, slows down, and stops moving. However, as it gets ''crowded in'' by other approaching walls, it moves out further in order to accompany them. Furthermore, it is also clear that as domain walls are pushed too close together their interaction becomes attractive leading to pair annihilation.

The behavior exhibited in Fig. 1 might be argued to result from the special set of initial conditions we have selected, namely, $\phi_i=\sqrt{a/2}$, $\forall i$. However, this is not the case. In Fig. 8 we show a bifurcation diagram for an identical set of parameters as in Fig. 1 but with continuous updating where the final configuration at a given value of A was used as initial conditions for the next value of A. This is more similar to the experimental situation where the field is slowly ramped up. As the field is increased the system explores various other states associated with many domain walls, since the system is no longer reset to a homogeneous state. However, the behavior remains the same as the complex and periodic re-

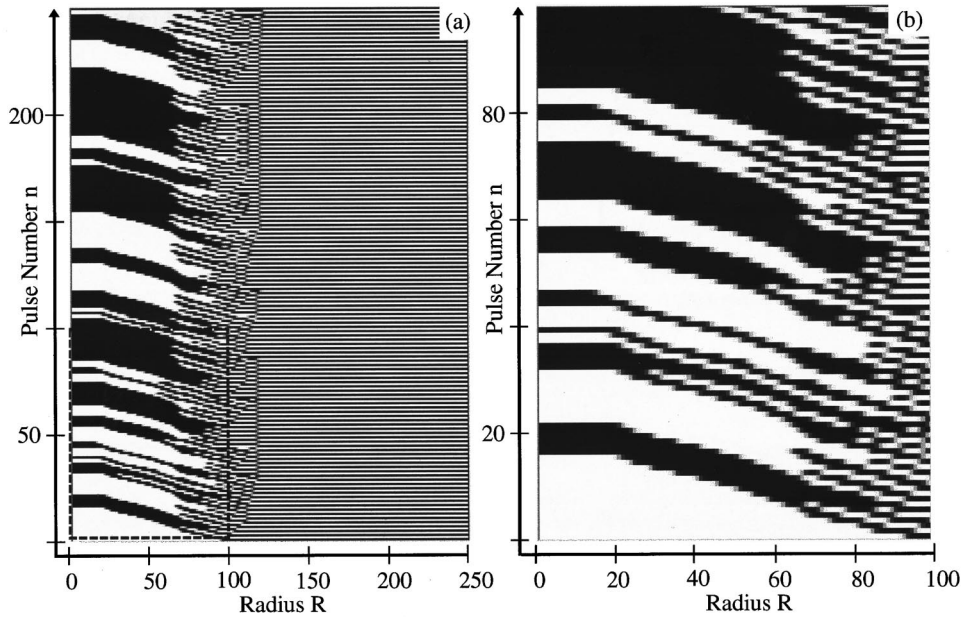

FIG. 7. (a) Space-time plot of the first complex regime for $R=1200$, $k=1$, $a=1.0$, $m=1.0$, $\gamma=0.25$, and $\sigma=0.3R$ at $A=1.82$. The horizontal direction (left to right) is the first 250 radial sites and the vertical direction (bottom to top) is time for the first 250 pulses. The plotted intensity is such that black corresponds to the positive well $(+\sqrt{2}/2)$ and white to the negative well $(-\sqrt{2}/2)$. (b) Closeup of the lower-left corner, as designated by the dashed lines in (a).

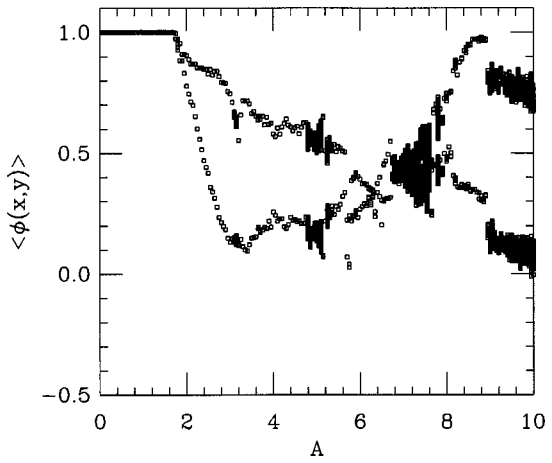

FIG. 8. Bifurcation diagram for the same set of system parameters as that of Fig. 1. Here, the system is continuously updated so that the final relaxed configuration for a given value of A was used as initial conditions for the next value of A. Periodic and complex regimes occur at identical values of A to that of Fig. 1.

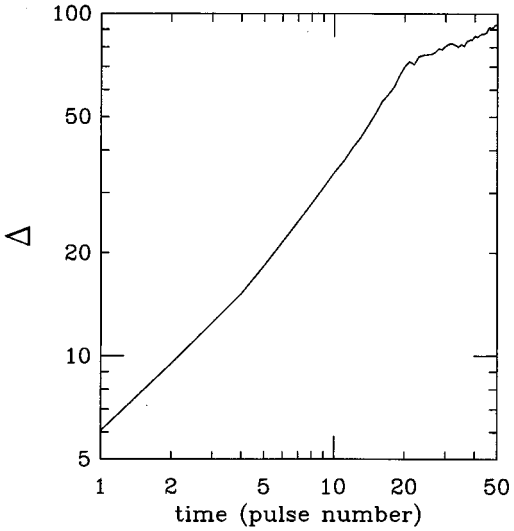

FIG. 9. Growth of small initial perturbations as a function of the number of pulses for the complex regime of $A=5.0$ in Fig. 1. The result has been averaged over 100 initially diverging perturbations. The data fits a power law behavior much better than an exponential function, suggestive of a zero Lyapunov exponent. The leveling off after the 20th pulse is due to the finite size of the ''chaotic'' region.

gimes occur for precisely the same range of values as that of Fig. 1. Although the final state of the system is dependent on its initial conditions, the qualitative behavior of the system is independent of them.

We have so far referred to the behavior of our system (shown in Fig. 7, for example) as ''complex.'' A natural question to ask is whether it is chaotic, i.e., does this system exhibit spatiotemporally chaotic behavior? One way to determine whether a system is chaotic is to measure a Lyapunov exponent. In the chaotic state, by definition, small deviations in the initial conditions grow exponentially with time, $\Delta \sim e^{\lambda t}$, so that a positive Lyapunov exponent λ is sufficient proof of chaos. In order to carry out such a study, we have defined the ''distance'' between two relaxed configurations as $\Delta=[\Sigma_{i=1}^{R_c}(\phi_i-\phi_i')^2]^{1/2}$, where ϕ_i' initially differs by a small amount from ϕ_i, and R_c is the radius of the complex zone. The initial perturbation ϕ_i' was obtained by moving a randomly chosen domain wall within the complex zone by one lattice site and then allowing for relaxation. Figure 9 shows a typical result of such a study after averaging over 100 diverging initial conditions. The complex regime is that of $A=5.0$ of Fig. 1. The initial divergence fits a power law, $\Delta \sim t^{\alpha}$ much better than an exponential. The leveling off after the 20th pulse is due to the finite size of the ''chaotic'' region. This behavior is reminiscent of complex systems displaying self-organized criticality (SOC) [13]. SOC systems are characterized by lack of time scale (as well as length scale) and thus exhibit power-law behavior. Therefore, initial perturbations grow algebraically instead of exponentially in SOC systems, suggestive of zero Lyapunov exponent [14]. Thus, SOC systems are at the edge of chaos. This type of behavior has also been referred to as ''weak chaos'' [15]. In fact, the dynamics of domain walls within the complex zone (e.g., that of Fig. 5) resembles certain one-dimensional sandpile models of SOC where energy is added at the left boundary and moves through the system in random motion to be dissipated at the right boundary. The possibility of this model and its variants exhibiting SOC is under current investigation. We have furthermore looked for other telltale signatures of a transition to chaos, such as a period-doubling sequence within the bifurcation diagrams similar to Fig. 1, and have found no evidence of such behavior.

We have also studied this model in spatial dimensions other than $d=2$. If we assume that the system is radially symmetric so that the only spatial variable is r, we may easily generalize Eq. (1) to d dimensions, which in the continuum form $[\phi_i(t)\rightarrow\phi(r,t)]$ reads

$$m\ddot{\phi}+\gamma\dot{\phi}=k\left[\frac{(d-1)}{r}\frac{d\phi}{dr}+\frac{d^2\phi}{dr^2}\right]-4\phi^3+2a\phi+F. \quad (3)$$

In Fig. 10 we show bifurcation diagrams for $d=1$ and $d=3$ for an identical set of parameters as in Fig. 1. In part (a) for $d=1$, the same type of periodic behavior as for $d=2$ is observed; however, in this case there is no ''chaotic'' regime. A periodic state characterized by a single domain wall simply leads to a periodic state with two domain walls as A is increased. On the other hand, in part (b) for $d=3$, the behavior is similar to the $d=2$ case, except that the ''chaotic'' regimes are now wider and more pronounced. This leads us to believe that the source of the observed complexity is not the usual nonlinear (ϕ^3) term, but the $(1/r)d\phi/dr$ in the diffusive term. Note that this term is zero everywhere except in the vicinity of domain walls, and it can thus be viewed as providing a long-range interaction between them. This term provides the ''pressure'' that a domain experiences from its neighboring (opposite) domain in a spherically symmetric geometry. This serves as a reminder of how different the complex high-dimensional behavior observed here is from the low-dimensional chaos observed in a single double-well oscillator [8].

Finally, we note that from an experimental point of view, it might be difficult to impart enough energy on the system to create a domain wall. It is therefore important to ask whether interesting dynamics can occur with subthreshold fields. We

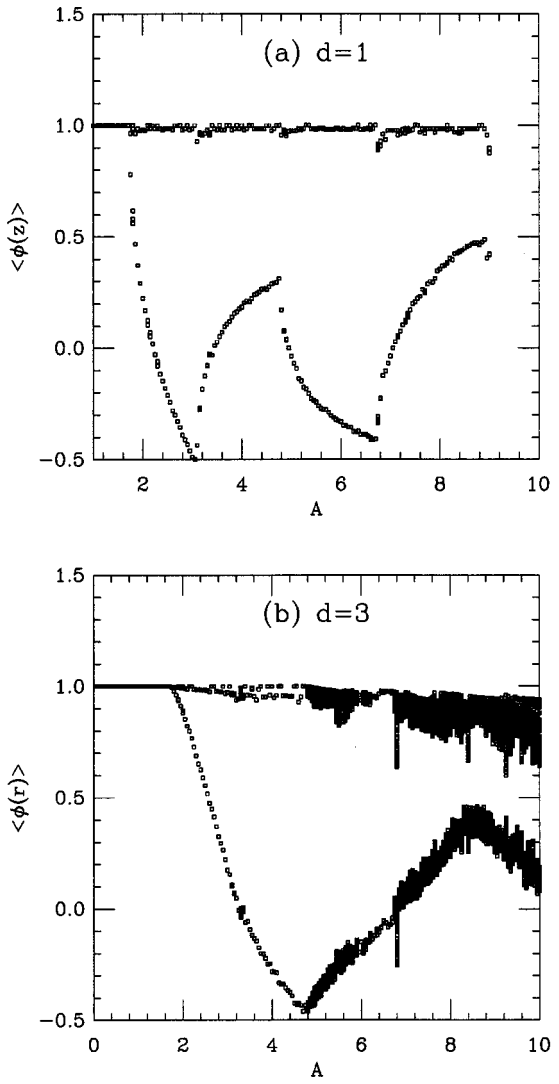

FIG. 10. Bifurcation diagram for the same set of parameters as that of Fig. 1, but in (a) $d=1$, and (b) $d=3$ (spherically symmetric). In part (a), only periodic behavior is observed while complexity becomes more pronounced for $d=3$.

have performed $1d$ simulations in the presence of a single domain wall (a kink or an antikink), and asked whether a subthreshold field with a strong gradient (small σ) can cause the domain wall to move around the sample. We observed that such domain walls could always be made to move around even with fields as small as half the threshold value. Figure 11 shows the result of such a run where a domain wall was placed near the middle of a $1d$ chain and a sharp subthreshold pulse was repeatedly applied in its proximity. As a result, the wall creeps towards the center of the pulse where the gradient is zero. The linear dependence in Figure 11 establishes the pulse gradient as the primary mechanism for domain wall dynamics. The discreteness of the lattice provides a pinning mechanism for domain walls, so that it takes a finite value of the pulse gradient to move a domain wall as seen from Fig 11. However, in the continuum limit the wall would move even for infinitesimal gradients. Also note that since the equation of motion [Eq. (1)] and the drive [Eq. (2)] are invariant under $\phi_i \rightarrow -\phi_i$, the dynamics of a kink or an antikink are the same under such situation, i.e.,

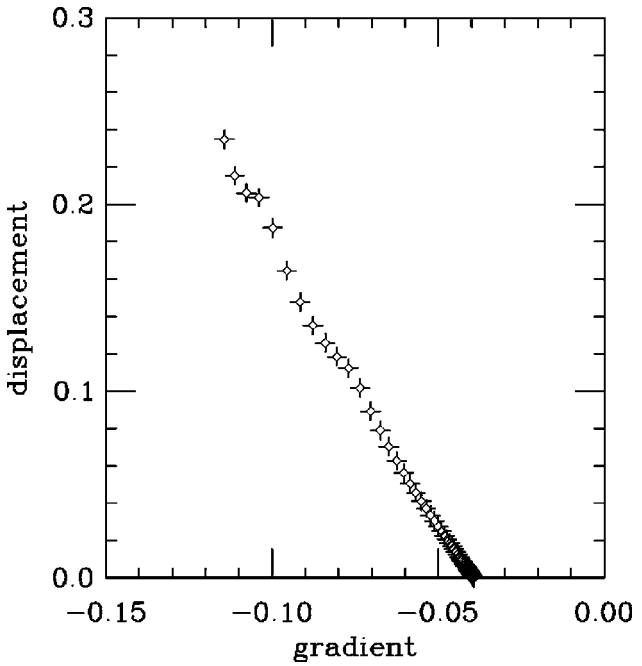

FIG. 11. Displacement of a single domain wall which results when a sharp subthreshold field of a given gradient is applied in its vicinity. Here, $d=1$, $N=500$, $k=10.0$, $a=2.0$, $\gamma=0.5$, $\sigma=5$, and $A=1.0$. The threshold for creating a new domain wall is $A=2.0$.

they both move towards the center of the pulse.

IV. CONCLUDING REMARKS

We have presented here results of our study for an extended, pulse-driven, model of double-well oscillators. The system models phonon dynamics in ferroelectrics under spatially varying ultrafast pulses. However, the model should also be of general interest as a generic extended dynamical system. As a result of the pulse gradient, with increasing pulse strength, stable domain walls are created, separating regions of opposite orientation. A bifurcation diagram is obtained, exhibiting both periodic and complex spatiotemporal behavior under repeated pulses. The periodic behavior is typically period-2 associated with successive creation and annihilation of bubbles and/or rings. The complex behavior, on the other hand, is associated with random creation and annihilation of many interacting domain walls. This complex regime belongs to a weakly chaotic class of extended systems characterized by zero Lyapunov exponent with algebraic growth of small initial perturbations. SOC systems have also been shown to be on the edge of chaos in the above sense. It is therefore an interesting question for future research to investigate the extent to which ideas behind SOC could be useful here.

We note that the overdamped ($m=0$) version of the extended double-well model has been previously studied in other contexts. Spatiotemporal stochastic resonance [16], for example, uses such a model in the presence of noise and a sinusoidal drive. The complexity observed here does not occur in the overdamped models, simply because complexity arises only when oscillators can jump their well more than once, which would be impossible in the absence of inertia. Furthermore, complexity does not occur in the one-

dimensional model because of the noninteracting nature of the domain walls.

Finally, we suggest that new experimental techniques such as near-field scanning optical microscopy may be useful in observing some of the effects discussed here.

ACKNOWLEDGMENTS

We would like to acknowledge many useful conversations with J. M. Carlson. This work was supported in part by the National Science Foundation Grant No. DMR-9701725.

[1] S. Fahy and R. Merlin, Phys. Rev. Lett. **73**, 1122 (1994).

[2] For a review of the properties of ferroelectrics, see M. E. Lines and A. M. Glass, *Principles and Applications of Ferroelectrics and Related Materials* (Clarendon, Oxford, 1977).

[3] T. P. Dougherty *et al.*, Science **258**, 770 (1992).

[4] H. J. Bakker, S. Hunsche, and H. Kurz, Phys. Rev. Lett. **69**, 2823 (1992).

[5] Y. Liu *et al.*, Phys. Rev. Lett. **75**, 334 (1995).

[6] P. M. Chaikin and T. C. Lubensky, *Principles of Condensed Matter Physics* (Cambridge University Press, Cambridge, 1995), Chap. 10.

[7] M. C. Cross and P. C. Hohenberg, Rev. Mod. Phys. **65**, 851 (1993).

[8] J. Guckenheimer and P. Holmes, *Nonlinear Oscillations, Dynamical Systems and Bifurcations of Vector Fields* (Springer-Verlag, New York, 1983), Chap. 1.

[9] W. H. Press, B. P. Flannery, S. A. Teukolsky, and W. T. Vetterling, *Numerical Recipes, The Art of Scientific Computing*, 2nd ed. (Cambridge University Press, Cambridge, 1995).

[10] G. Shirane, Rev. Mod. Phys. **46**, 437 (1974).

[11] Sometimes the new domain wall does not reach the original one to annihilate it. Instead, it simply sits nearby, creating a thin ''ring'' in the system. The effect of this behavior is the apparent ''noisiness'' in the upper branch of the bifurcation diagram where $\langle\phi\rangle$ becomes smaller than its homogeneous $\sqrt{a/2}$ value.

[12] We note that at $A=5.8$ a ''quasiperiodic'' state emerges, which the system reaches after about 50 pulses. Here, a fixed number of domain walls (10), occupying a zone near the center, move around by small amounts after each pulse, while the rest of the system executes a period-2 motion. We consider this atypical behavior.

[13] P. Bak, C. Tang, and K. Wiesenfeld, Phys. Rev. Lett. **59**, 381 (1987).

[14] K. Chen, P. Bak, and S. P. Obukhov, Phys. Rev. A **43**, 625 (1991).

[15] P. Bak and K. Chen, in *Fractals and Their Application to Geology*, edited by C. C. Barton and P. R. LaPointe (Geological Society of America, Denver, 1991).

[16] F. Marchesoni, L. Gammaitoni, and A. R. Bulsara, Phys. Rev. Lett. **76**, 2609 (1996).